

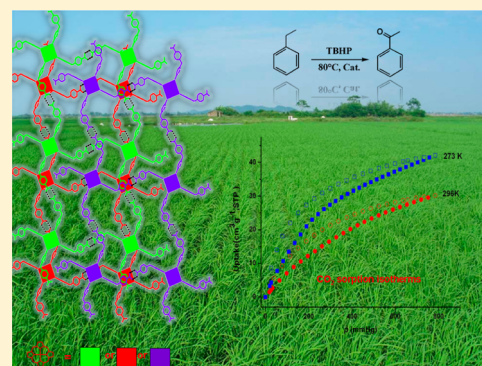
Permanently Porous Co(II) Porphyrin-Based Hydrogen Bonded Framework for Gas Adsorption and Catalysis

Zengqi Zhang, Jun Li,* Yahong Yao, and Shu Sun

Key Laboratory of Synthetic and Natural Functional Molecule Chemistry of Ministry of Education, College of Chemistry and Materials Science, Northwest University, Xi'an, Shaanxi 710069, People's Republic of China

Supporting Information

ABSTRACT: A new microporous hydrogen-bonded organic framework (HOF) based on a cobalt(II) porphyrin, namely, Co(II) 5,10,15,20-tetra(4-(4-acetateethyl)phenoxy)phenylporphyrin (**1**), has been synthesized and structurally characterized. Single crystal X-ray diffraction analysis reveals that porphyrin molecules connect each other by intermolecular hydrogen bonds to form 2D layer, and the 2D layer further links through $\pi \cdots \pi$ interactions to form 3D supramolecular structure, exhibiting one kind of micropore with $3.98 \times 6.47 \text{ \AA}^2$. The HOF of **1** exhibits not only a permanent porosity with the Langmuir surface areas of $158.79 \text{ m}^2 \cdot \text{g}^{-1}$, and the Brunauer–Emmett–Teller surface areas of $97.70 \text{ m}^2 \cdot \text{g}^{-1}$, but also, more importantly, high catalytic efficiency and selectivity for oxidation of ethylbenzene to acetophenone in quantitative 83.1% yield.



1. INTRODUCTION

Because porous materials have very important and useful application in gas storage, separation, catalysis, and electrodes,^{1–5} they have attracted extensive research attention to target such materials for highly efficient gas storage and catalysis. Such efforts eventually lead to the emergence of porous metal organic frameworks (MOFs). During the past two decades, a lot of porous MOFs have been prepared by self-assembly of metal and organic ligand, such as excellent work by the Xiaoming Chen group and the Jing Li group in such areas in the past years.^{6–15} Compared with MOFs, porous hydrogen-bonded organic frameworks (HOFs) have lagged significantly behind. HOFs, which are quite different from MOFs, are directly self-assembled from organic building blocks via weak hydrogen-bonding interactions. Although HOFs have been proposed as potential porous materials for about the past two decades as well,^{16,17} only very few HOFs exhibiting permanent porosity have been reported in recent years.^{18–23} Such a situation is mainly due to hydrogen-bonding interactions which are typically too weak to stabilize the frameworks and establish permanent porosities. In other words, the supermolecular structure is usually broken and HOFs collapse when solvent guests are removed. Unlike MOFs, HOFs have advantages of solution processability and easy purification and can be easily recovered by recrystallization, making them promising functional materials.

Porphyrin is a typical functional discotic molecule and its properties can be easily modified by introduction of peripheral substituent in porphyrin and insertion of metal atoms into the center of the porphyrin ring.^{24,25} In the past decade, porphyrin has attracted great research attention as a versatile synthetic base for various materials due to their rich electronic, catalytic

property, and strong optical absorption and emission.^{26–33} Because of their desirable functional properties, porphyrins have been ideal building blocks for construction of functional MOFs, and hundreds of porphyrin based MOFs have been reported from the 1990s.^{34–44} Although porphyrin supermolecular structure connected by hydrogen-bonding interactions have been widely studied,^{45–48} porphyrin based HOF exhibiting permanent porosity had not been studied until 2015 when Banglin Chen reported a HOF constructed by 2,4-diaminotriazinyl functionalized porphyrin compound; to the best of our knowledge, this is the only reported porphyrin based HOF.⁴⁹ Herein, we report a new porphyrin-based HOF **1** constructed from Co(II) 5,10,15,20-tetra(4-(4-acetateethyl)phenoxy)phenylporphyrin (CoTCPp) and permanent porosity of **1** was confirmed by gas sorption isotherms. In addition, catalytic activity to ethylbenzene oxidation of HOF **1** was first evaluated.

2. EXPERIMENTAL SECTION

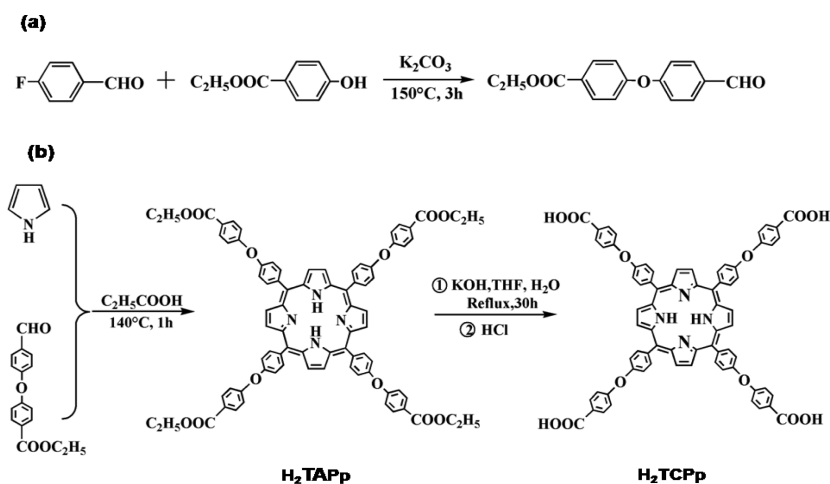
2.1. Materials and Instruments. 4-Fluorobenzaldehyde and ethyl-*p*-hydroxybenzoate were purchased from Sigma-Aldrich Japan (Chiba, Japan); other reagents were purchased from Beijing Chemical Reagents Company; all solvents and reagents were used without further purification, except pyrrole, which was distilled before use.

IR spectra were obtained with samples in KBr for the title complexes on a BEQUZNDX-550 series FT-IR spectrophotometer in the range $4000\text{--}400 \text{ cm}^{-1}$. UV–vis spectra were performed by a Shimadzu UV1800 UV–vis spectrophotometer. ¹H NMR spectra were collected in deuterated chloroform (CDCl₃) using a Bruker AC-400 at

Received: July 14, 2015

Revised: September 2, 2015

Scheme 1. (a) Syntheses of the 4-(4-Formylphenoxy)ethylbenzoate. (b) Syntheses of 5,10,15,20-Tetra(4-(4-acetateethyl)phenoxy)phenyl porphyrin (H_2TAPP) and 5,10,15,20-Tetra(4-(4-carboxyl)phenoxy)phenyl porphyrin (H_2TCPp)



room temperature and chemical shifts were reported in ppm units with respect to the reference frequency of TMS. Mass spectrometry (MS) analysis was carried out on a matrix assisted laser desorption/ionization time-of-flight mass spectrometer (MALDI-TOF MS, Krato Analytical Company of Shimadzu Biotech, Manchester, Britain) using a standard procedure involving 1 mL of the sample solution.

2.2. Synthesis. The synthetic routes to the porphyrin and metalloporphyrins are shown in Scheme 1.

2.2.1. Synthesis of 4-(4-Formylphenoxy)ethylbenzoate. The synthetic method used in our study was presented in the previous report.⁵⁰ In a 100 mL three-necked flask, ethyl-*p*-hydroxybenzoate (17 mmol), 4-fluorobenzaldehyde (17 mmol), and K_2CO_3 reacted in refluxing 30 mL *N,N*-dimethylformamide (DMF) for 3 h. After being cooled to room temperature, the reaction mixture was quenched with water and extracted with CH_2Cl_2 . The organic layer was washed with water, dried over Na_2SO_4 , and evaporated. The desired solid was obtained. Yield: 52%. MS: m/z 271.10 ($[M + H]^+$) amu. Mp: 55 °C. FT-IR: ν , cm^{-1} , 3420, 2848, 2753, 1721, 1396, 1367, 1236, 1167, 1097, 836, 698.

2.2.2. Synthesis of 5,10,15,20-Tetra(4-(4-acetateethyl)phenoxy)phenyl porphyrin (H_2TAPP). The synthetic method used in our study was the well-known Adler-Longo method.⁵¹ 4-(4-Formylphenoxy)ethylbenzoate (12 mmol) and pyrrole (12 mmol) were reacted in refluxing propionic acid for 50 min. The crude product was purified on a silica-gel column with dichloromethane as eluent, and a desired purple solid of compound H_2TAPP was obtained. Yield: 6.2%. Mp: >250 °C, UV-vis (CH_2Cl_2): λ_{max}/nm , 418 (Soret band), 515, 551, 585, 650 (Q bands). FT-IR: ν , cm^{-1} , 1711, 1587, 1500, 1231, 1160, 1098, 967, 874, 797. Anal. Calcd (found) for $C_{80}H_{62}N_4O_{12}$ (mol wt 1270.44) %: C, 75.58 (75.54); H, 4.92 (4.93); N, 4.41 (4.45). MS: m/z 1271.40 ($[M + H]^+$) amu. 1H NMR ($CDCl_3$, 400 MHz): δ , ppm 8.95 (s, 8H, β position of the pyrrole moiety), 8.22 (dd, $J = 14.6$, 8.3 Hz, 14H, Ar), 7.41 (dd, $J = 48.4$, 8.2 Hz, 18H, Ar), 4.43 (dd, $J = 14.0$, 6.9 Hz, 8H, $-CH_2-$), 1.45 (t, $J = 7.0$ Hz, 12H, $-CH_3$), -2.75 (s, 2H, NH).

2.2.3. Synthesis of 5,10,15,20-Tetra(4-(4-carboxyl)phenoxy)phenyl porphyrin (H_2TCPp). H_2TAPP (0.1 g) was dissolved in 15 mL tetrahydrofuran, and 20 mL alkaline aqueous solution (KOH, 1 mol/L) was added. Then the mixture was stirring under reflux for 30h. After being cooled to room temperature, HCl was added and the desired solid powder precipitated. Yield: 6.2%. Mp: > 250 °C, UV-vis (CH_2Cl_2): λ_{max}/nm , 419 (Soret band), 516, 550, 592, 648 (Q bands). FT-IR: ν , cm^{-1} , 3029, 1708, 1597, 1498, 1236, 1164, 1093, 967, 874, 797. Anal. Calcd (found) for $C_{72}H_{46}N_4O_{12}$ (mol. wt: 1158.31), %: C, 74.60 (74.57); H, 4.00 (4.02); N, 4.41 (4.47). MS: m/z 1157.30 ($[M - H]^-$) amu.

2.2.4. Synthesis of $[Co(C_{72}H_{44}N_4O_{12})] \cdot 2DMF$ (1**).** 7 mg H_2TCPp and 10 mg $CoCl_2$ was dissolved in 2 mL DMF and 1 mL $HCOOH$,

and then the solution was added in a polytetrafluoroethylene lined stainless steel container. The container was gradually heated to 150 °C in 4 h and kept for 3 days, then the crude products gradually cooled to room temperature. The desired purple crystal $[Co(C_{72}H_{44}N_4O_{12})] \cdot 2DMF$ (**1**) was obtained in 67% yield. Calcd for $C_{78}H_{44}CoN_6O_{14}$: C, 69.49; H, 3.29; N, 6.23%. Found: C, 69.57; H, 3.34; N, 6.27%. UV-vis-DRS: λ_{max}/nm , 423 (Soret band), 535 (Q-band). IR spectrum (KBr, ν/cm^{-1}): 1643, 1400, 1236, 1164, 998, 803, 768.

2.2.5. Crystallographic Data Collection and Refinement. The crystallographic data of **1** were obtained at 173 K with a Bruker SMART CCD diffractometer with graphite monochromated Mo $K\alpha$ radiation ($\lambda = 0.71073$ Å). Absorption corrections were applied using SADABS program.⁵² The structure was solved by direct method and refined by full-matrix least-squares techniques using the SHELXL-97 program.⁵³ Anisotropic thermal parameters were assigned to all non-hydrogen atoms. Hydrogen atoms were placed in geometrically calculated positions.

2.2.6. Typical Procedure Catalytic Oxidation. A mixture of alkylbenzene (0.1 mmol), *tert*-butylhydroperoxide (TBHP, 0.5 mmol), catalyst (0.005 mmol), and acetonitrile (2.0 mL) was stirred at 80 °C for 20 h. After the reaction, the identity of the product was determined by using gas chromatography (GC), compared with the authentic samples analyzed under the same conditions. The yield of product was also obtained by GC analysis with a flame-ionization detector (FID) using a capillary SE-54 column.

3. RESULTS AND DISCUSSION

3.1. Crystal Structure. Single-crystal X-ray diffraction analysis reveals that **1** belongs to the triclinic system with space group $P\bar{1}$. As shown in Figure 1, Co(II) coordinates with four N atoms of porphyrin to form a square geometry. The distance of Co–N [1.96(7)–1.97(7) Å] are in the normal range for the similar porphyrin based Co(II) compounds,^{54,55} and slight longer than Co–N length in Co(III) porphyrin crystal.⁵⁶ The displacement of each 20-membered ring atom is in the range of $-0.057(3)$ to $+0.057(3)$ Å from the equatorial mean N4 plane, while that of four pyrrole N atoms is 0 Å from their mean N4 plane, indicating that atoms of porphyrin macrocycle are perfectly coplanar.

In structure **1**, each Co(II) porphyrin molecule connects with four other porphyrin molecules through hydrogen bond interactions formed by carboxy groups of two porphyrins, and Co(II) porphyrin molecules are further self-assembled into a two-dimensional (2D) supramolecular layer (Figure 2a). The neighboring layers are packed into a 3D framework via the

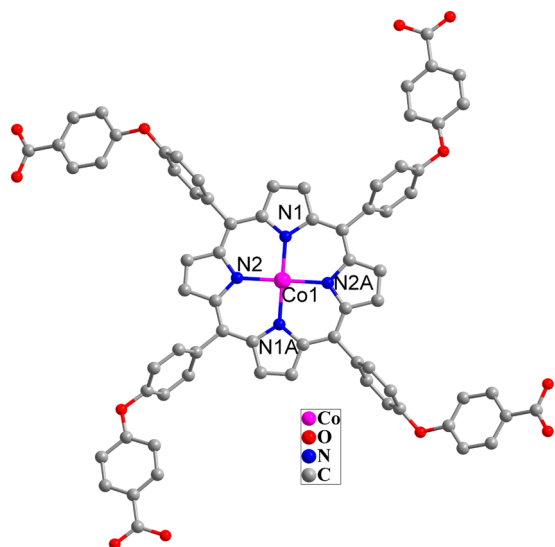


Figure 1. Molecular structure of the organic building block for construction of **1**.

intermolecular C–H $\cdots\pi$ interactions between phenyl and porphyrin macrocycle (shown in Figure 2b), generating a microporous structure with the pore size of 3.98×6.47 Å (Figure 2c,d). If one considers the porphyrin building block to be a four-connected node in the square geometry, the net of **1** can then be rationalized as a $sql\{4^46^2\}$ network topology (Figure S1, Supporting Information). The potential solvent accessible void space accounts for approximately 18.90% of the whole crystal volume as estimated by PLATONN.

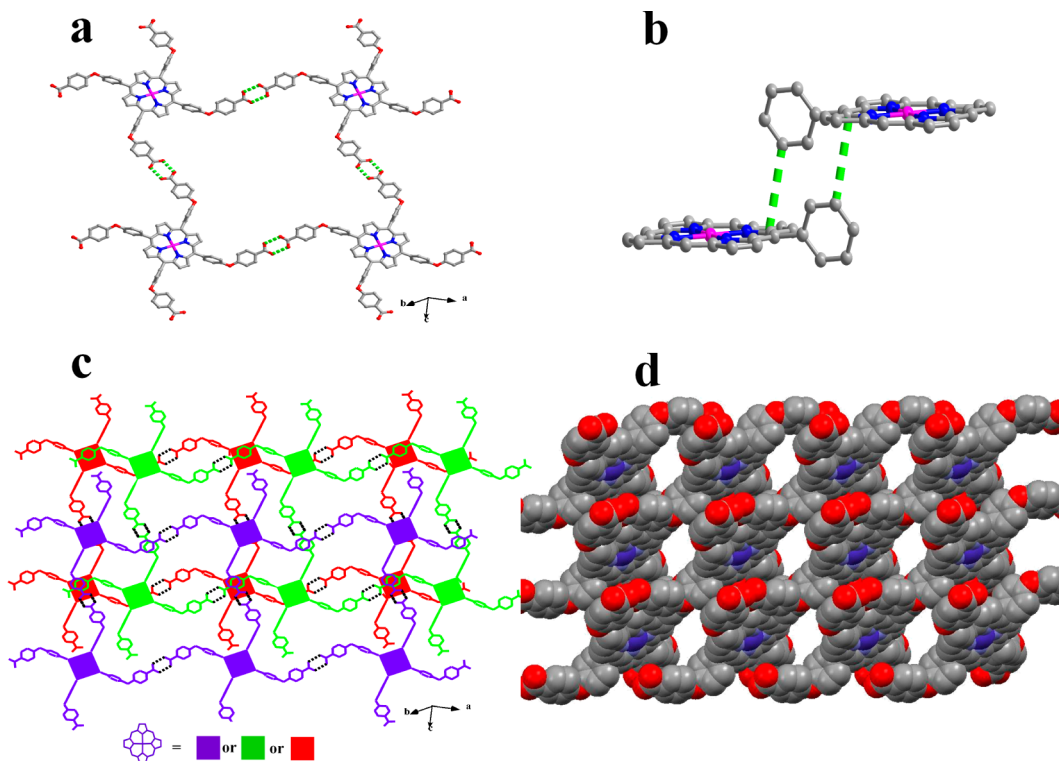


Figure 2. (a) Hydrogen bond interaction in structure of **1** (hydrogen atoms were omitted for clarity; the hydrogen bonds were shown as dotted line). (b) Intermolecular $\pi\cdots\pi$ interaction between two porphyrin molecules (peripheral substituents were omitted for clarity; the C–H $\cdots\pi$ interactions were shown as dotted line). (c) 3D packing framework. (d) Rhombic channels in **1** view along the a axis with an approximate dimension of 3.98×6.47 Å².

3.2. Powder XRD and Thermogravimetric Analysis.

The phase purity for **1** is confirmed by powder X-ray diffraction (PXRD) analysis in bulk (Figure 3). The evacuated samples are

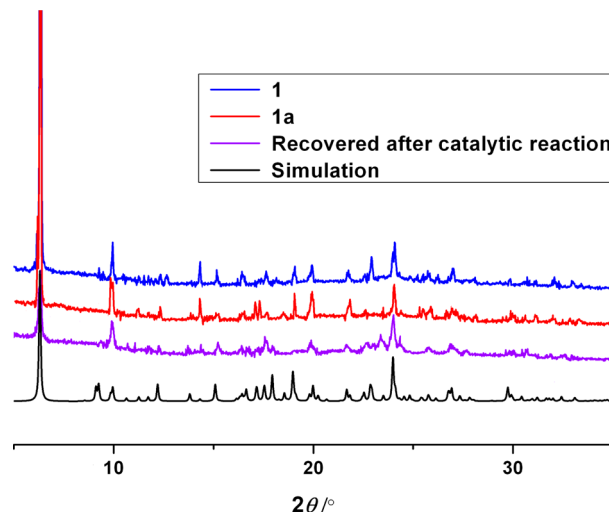


Figure 3. Powder X-ray diffraction patterns of **1**, **1a**, and recovered **1**.

obtained through heating under vacuum at 80 °C for 8 h. PXRD results show that all of the measured peaks closely matched those in the simulated pattern generated from the single-crystal XRD data, indicating that after being heated for 8 h, **1** retains the crystalline nature and porous structure with the pores comparable to those revealed in the single crystal. To study the thermal stability of **1**, thermogravimetric analysis

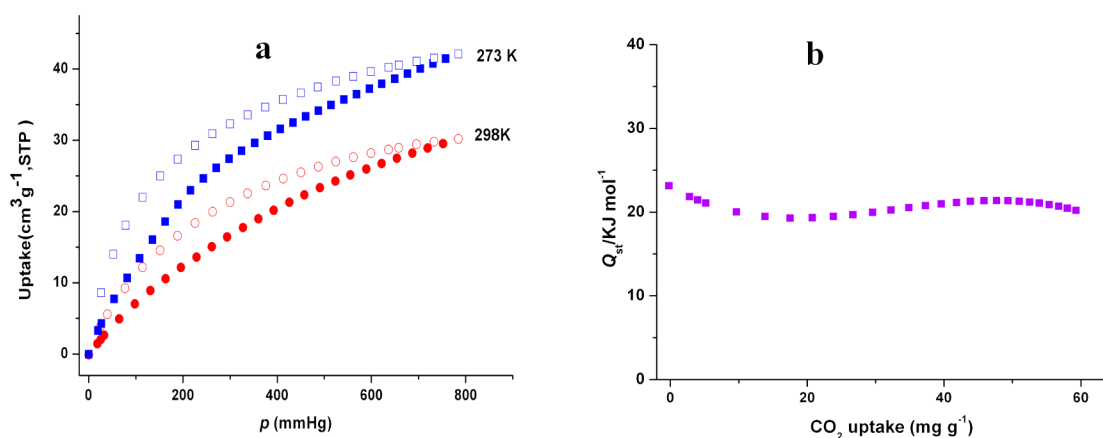


Figure 4. (a) CO₂ sorption isotherms of **1a** at 273 and 298 K (solid symbols: adsorption; open symbols: desorption). (b) Isosteric heat of CO₂ adsorption for **1a** estimated by the virial equation.

Table 1. Selective Oxidation of Alkylbenzenes Catalyzed by Porphyrins

| Entry | Substrate | Catalyst | Product | Conv.(%) | Select. (%) |
|-------|-----------|----------------------|---------|----------|-------------|
| 1 | | 1 | | 83.1 | > 99 |
| 2 | | 1^c | | 76.2 | > 99 |
| 3 | | 1^d | | 72.7 | > 99 |
| 4 | | 1 | | 35.8 | > 99 |
| 5 | | 1 | | 24.8 | > 99 |
| 6 | | 1 | | 75.1 | 74.2 |
| 7 | | CoCl ₂ | | 5 | 71 |
| 8 | | no | | trace | - |

^aConditions: a mixture of catalyst (0.005 mmol), alkylbenzene (0.1 mmol), and TBHP (0.5 mmol) in acetonitrile (2.0 mL) was stirred at 80 °C for 20 h. ^bBased on GC analysis. ^cThird cycle. ^dSixth cycle.

(TGA, Figure S2 in Supporting Information) is carried out in the temperature range from 25 to 800 °C under a flow of N₂ with a heating rate of 10 °C·min⁻¹. Thermogravimetric analysis of **1** reveals that there is a weight loss of 10.05% from room temperature to 220 °C, corresponding to two guest *N,N*-dimethylformamide (DMF) molecules in the pore of **1**. Then, the curve is followed by a relatively steady platform up to 400 °C; after this, the framework starts to decompose.

Before performing the adsorption property test, the guest DMF molecules in **1** are removed by solvent exchange with acetone; and the resulting samples are further activated at 80 °C to generate the activated HOF material (**1a**). The TGA curve of **1a**, shown in Figure S2 of the Supporting Information,

shows that there is a platform without weight loss in the temperature range from room temperature to 400 °C, indicating all solvent molecules have been removed. The PXRD pattern of **1a** (Figure 3) is only slightly shifted from that of the as-synthesized **1** crystal, which is the result of the flexibility and shrinkage of the framework. The PXRD data indicate that the desolvated framework is obtained.

3.3. Gas Adsorption. To confirm the permanent microporosity of the HOF **1a**, gas-adsorption measurements (N₂ and CO₂) of **1a** was performed. The N₂ sorption experiment of **1a** at 77 K shows type I adsorption isotherm behavior (Figure S3) with apparent Langmuir surface areas of 158.79 m²·g⁻¹ and Brunauer–Emmett–Teller (BET) surface areas of 97.70 m²·g⁻¹.

g^{-1} , respectively. The BET surface area of **1a** is slightly smaller than those microporous porphyrin-based MOFs with the 2D layered configurations.^{57,58} There is adsorption–desorption hysteresis on the N_2 sorption curve, indicating the existence of micropores in **1a**. The experimental pore size distribution (PSD) is shown in Figure S4 of Supporting Information. The median pore width is 0.99 nm and maximum pore volume is $0.052 \text{ cm}^3 \cdot \text{g}^{-1}$.

The CO_2 sorption properties on desolvated **1a** at two different temperatures (273 and 298 K) were also evaluated. As shown in Figure 4a, the CO_2 adsorption isotherms of **1a** at both 273 and 298 K are nonclassical type I adsorption isotherms and the CO_2 uptakes are $42.18 \text{ cm}^3 \cdot \text{g}^{-1}$ (8.28 wt %) and $30.19 \text{ cm}^3 \cdot \text{g}^{-1}$ (5.93 wt %) at 273 and 298 K, respectively. It is obvious that the final CO_2 uptake values of **1a** at both 273 and 298 K are higher than reported porphyrin based HOF,⁴⁹ which is comparable to some previously reported MOFs.⁵⁹ All sorption isotherms of **1a** at 273 and 298 K show hysteresis. In order to further study gas sorption behaviors of **1a**, the adsorption enthalpy of the HOF **1a** to CO_2 molecules (Figure 4b) was calculated according to the CO_2 gas adsorption isotherms at 273 and 298 K, utilizing a built-in function in Micromeritics ASAP 2020 analyzer based on the Virial equation (shown in the Figure S5, Supporting Information). The fitted enthalpy of CO_2 adsorption for **1a** at zero coverage is $23.20 \text{ kJ} \cdot \text{mol}^{-1}$, which is comparable to those found in MOFs with small pores.⁶⁰

3.4. Catalytic Activity of 1. We examined **1** for its catalytic oxidation to ethylbenzene. The ethylbenzene oxidation was performed in solvent of acetonitrile at 80°C using *tert*-butylhydroperoxide (TBHP) as the oxidant, with GC monitored throughout the reaction. The results (Table 1) show that **1** efficiently catalyzes the conversion of ethylbenzene to the only product acetophenone quantitatively in 83.1% yield. After reaction finished, solid **1** was easily recovered by centrifuging and filtration (Figure S6 of Supporting Information) and subsequently used in successive runs with only slightly decreased product yields. The conversion after six cycles is 72.7%. When the substrate was changed to 1-phenylpropane, 1,2,3,4-tetrahydronaphthalene, and diphenylmethane, the conversion was decreased to 35.8%, 75.1%, and 24.8%, respectively. There is no obvious change in the P-XRD pattern (Figure 3) except that peaks at $2\theta = 19^\circ$ and $2\theta = 21^\circ$ disappeared in the curve of recovered **1**, indicating that the framework and pore are kept after the reaction.

4. CONCLUSION

In summary, we have successfully constructed a new microporous hydrogen-bonded organic framework **1** from porphyrin building block (Co(II) 5,10,15,20-tetra(4-(4-acetateethyl)phenoxy)phenylporphyrin). **1** is thermally stable, as well as stable in common solvent. Its permanent porosities have been confirmed not only by the 3D porous structure, but, more importantly, by its gas sorption isotherms. In addition, the catalytic oxidation results show that **1** displays high catalytic activity with the only product acetophenone quantitatively in 83%, and after three cycles the catalytic activity slightly decreases. These unique features of **1**, including the exceptional stability, adsorption for CO_2 , and high catalytic activity, make it outstanding among the HOFs reported in the literature.

■ ASSOCIATED CONTENT

Supporting Information

Refer to CCDC 1411460 for crystallographic data in CIF format. The Supporting Information is available free of charge on the ACS Publications website at DOI: 10.1021/acs.cgd.5b00987.

TGA, N_2 sorption isotherms, crystallographic data (PDF)

■ AUTHOR INFORMATION

Corresponding Author

*E-mail: junli@nwu.edu.cn.

Notes

The authors declare no competing financial interest.

■ ACKNOWLEDGMENTS

This work has been supported by the NNSF (No. 21271148). We are very grateful to Shaanxi Normal University for their kind assistance.

■ REFERENCES

- (1) Sanna, A.; Kuusik, G. R. *Chem. Soc. Rev.* **2014**, *43*, 8049–8080.
- (2) Linares, N.; Silvestre-Albero, A. M.; Serrano, E.; Silvestre-Albero, J.; García-Martínez, J. *Chem. Soc. Rev.* **2014**, *43*, 7681–7717.
- (3) Rolison, D. R. *Chem. Rev.* **1990**, *90*, 867–878.
- (4) Khajeh, M.; Laurent, S.; Dastafkan, K. *Chem. Rev.* **2013**, *113*, 7728–7768.
- (5) Wu, D. C.; Xu, F.; Sun, B.; Fu, R. W.; He, H. K. *Chem. Rev.* **2012**, *112*, 3959–4015.
- (6) He, C. T.; Jiang, L.; Liao, P. Q.; Zhang, J. P.; Chen, X. M. *J. Am. Chem. Soc.* **2015**, *137*, 7217–7223.
- (7) Qi, X. L.; Liu, S. Y.; Lin, R. B.; Zhang, J. P.; Chen, X. M.; et al. *Chem. Commun.* **2013**, *49*, 6864–6866.
- (8) Zhang, J. P.; Zhang, Y. B.; Lin, J. B.; Chen, X. M. *Chem. Rev.* **2012**, *112*, 1001–1033.
- (9) Zhang, J. P.; Zhu, A. X.; Chen, X. M. *Chem. Commun.* **2012**, *48*, 11395–11397.
- (10) Nijem, N.; Wu, H.; Canepa, P.; Li, J.; et al. *J. Am. Chem. Soc.* **2012**, *134*, 15201–15204.
- (11) Hu, Z.; Pramanik, S.; Tan, K.; Li, J.; et al. *Cryst. Growth Des.* **2013**, *13*, 4204–4207.
- (12) Hu, Z.; Deibert, B. J.; Li, J. *Chem. Soc. Rev.* **2014**, *43*, 5815–5840.
- (13) Pramanik, S.; Zheng, C.; Zhang, X.; Li, J.; et al. *J. Am. Chem. Soc.* **2011**, *133*, 4153–4155.
- (14) Lan, A.; Li, K.; Wu, H.; Ki, W.; Hong, M. C.; Li, J.; et al. *Angew. Chem., Int. Ed.* **2009**, *48*, 2334–2338.
- (15) Li, B.; Zhang, Z.; Li, Y.; Yao, K.; Shi, Z.; Li, J.; et al. *Angew. Chem., Int. Ed.* **2012**, *51*, 1412–1415.
- (16) Simard, M.; Wuest, J. D.; et al. *J. Am. Chem. Soc.* **1991**, *113*, 4696–4698.
- (17) Cooper, A. I. *Angew. Chem., Int. Ed.* **2012**, *51*, 7892–7894.
- (18) Luo, X. Z.; Jia, X. J.; Deng, J. H.; Wang, K. J.; Zhong, D. C.; et al. *J. Am. Chem. Soc.* **2013**, *135*, 11684–11687.
- (19) Mastalerz, M.; Oppel, I. M. *Angew. Chem., Int. Ed.* **2012**, *51*, 5252–5255.
- (20) He, Y.; Xiang, S.; Chen, B. *J. Am. Chem. Soc.* **2011**, *133*, 14570–14573.
- (21) Li, P.; He, Y.; Zhao, Y.; Weng, L.; Chen, B.; et al. *Angew. Chem., Int. Ed.* **2015**, *54*, 574–577.
- (22) Li, P.; He, Y.; Arman, H. D.; Wang, H.; Chen, B.; et al. *Chem. Commun.* **2014**, *50*, 13081–13084.
- (23) Li, P.; He, Y.; Guang, J.; Weng, L.; Chen, B.; et al. *J. Am. Chem. Soc.* **2014**, *136*, 547–549.
- (24) Jasat, A.; Dolphin, D. *Chem. Rev.* **1997**, *97*, 2267–2340.

- (25) Drain, C. M.; Varotto, A.; Radivojevic, I. *Chem. Rev.* **2009**, *109*, 1630–1658.
- (26) Iengo, E.; Gatti, T. M.; Indelli, T.; Alessio, E.; et al. *Chem. Commun.* **2011**, *47*, 1616–1618.
- (27) Alessio, E.; Casanova, M.; Zangrando, E.; et al. *Chem. Commun.* **2012**, *48*, 5112–5114.
- (28) Yoshimoto, S.; Sawaguchi, T.; Kobayashi, N.; et al. *Angew. Chem., Int. Ed.* **2007**, *46*, 1071–1074.
- (29) Iengo, E.; Zangrando, E.; Alessio, E. *Acc. Chem. Res.* **2006**, *39*, 841–851.
- (30) Che, C. M.; Huang, J. S. *Chem. Commun.* **2009**, *45*, 3996–4015.
- (31) Lai, T. S.; Zhang, R.; Che, C. M.; et al. *Chem. Commun.* **1998**, *34*, 1583–1584.
- (32) Zhang, R.; Yu, W. Y.; Che, C. M.; et al. *Chem. Commun.* **1999**, *35*, 1791–1792.
- (33) Jiang, G. X.; Chen, J.; Thu, H. Y.; Huang, J. S.; Che, C. M.; et al. *Angew. Chem., Int. Ed.* **2008**, *47*, 6638–6642.
- (34) Abrahams, B. F.; Hoskins, B. F.; Michail, D. M.; Robson, R. *Nature* **1994**, *369*, 727–729.
- (35) Farha, O. K.; Shultz, A. M.; Sarjeant, A. A.; Hupp, J. T.; et al. *J. Am. Chem. Soc.* **2011**, *133*, 5652–5655.
- (36) Wang, T. C.; Bury, W.; Stoddart, J. F.; Hupp, J. T.; Farha, O. K.; et al. *J. Am. Chem. Soc.* **2015**, *137*, 3585–3591.
- (37) Zou, C.; Zhang, T. F.; Yan, L. J.; Wu, C. D.; et al. *Inorg. Chem.* **2013**, *52*, 3620–3626.
- (38) Yang, X. L.; Wu, C. D. *Inorg. Chem.* **2014**, *53*, 4797–4799.
- (39) Yang, X. L.; Xie, M. H.; Zou, C.; Wu, C. D.; et al. *J. Am. Chem. Soc.* **2012**, *134*, 10638–10645.
- (40) Liu, T. F.; Feng, D. W.; Chen, Y. P.; Zhou, H. C.; et al. *J. Am. Chem. Soc.* **2015**, *137*, 413–419.
- (41) Feng, D.; Chung, W. C.; Wei, Z.; Gu, Z. Y.; Zhou, H. C.; et al. *J. Am. Chem. Soc.* **2013**, *135*, 17105–17110.
- (42) George, S.; Goldberg, I. *Cryst. Growth Des.* **2006**, *6*, 2651–2654.
- (43) Park, J.; Feng, D. W.; Yuan, S.; Zhou, H. C. *Angew. Chem., Int. Ed.* **2015**, *54*, 430–435.
- (44) Guo, Z. Y.; Yan, D.; Wang, H. L.; Li, X. L.; Chen, B.; et al. *Inorg. Chem.* **2015**, *54*, 200–204.
- (45) Goldberg, I.; Vinodu, M. *CrystEngComm* **2004**, *6*, 215–220.
- (46) George, S.; Goldberg, I. *Cryst. Growth Des.* **2006**, *6*, 755–762.
- (47) Chen, W.; El-khouly, M. E.; Fukuzumi, S. *Inorg. Chem.* **2011**, *50*, 671–678.
- (48) Zhang, Z.; Duan, Y.; Li, J. *Inorg. Chem. Commun.* **2015**, *58*, 53–56.
- (49) Yang, W.; Li, B.; Wang, H.; Alduhaish, O.; Chen, B.; et al. *Cryst. Growth Des.* **2015**, *15*, 2000–2004.
- (50) Nishizawa, R.; Nishiyama, T.; Hisaichi, K.; Hirai, K.; et al. *Bioorg. Med. Chem.* **2010**, *18*, 5208–5223.
- (51) Osati, S.; Safari, N.; Jamaat, P. R. *Inorg. Chim. Acta* **2010**, *363*, 2180–2184.
- (52) Sheldrick, G. M. *SADABS, Program for Area Detector Adsorption Correction*; Institute for Inorganic Chemistry; University of Gottingen, Germany, 1996.
- (53) Sheldrick, G. M. *SHELX-97 Program for the Solution of Crystal Structures*; University of Goettingen: Germany, 1997.
- (54) Choi, E. Y.; Barron, P. M.; Novotny, R. W.; Hu, C.; Choe, W. *Inorg. Chem.* **2009**, *48*, 426–428.
- (55) Kosal, M. E.; Chou, J. H.; Wilson, S. R.; Suslick, K. S. *Nat. Mater.* **2002**, *1*, 118–121.
- (56) Adachi, H.; Suzuki, H.; et al. *Inorg. Chem.* **2002**, *41*, 2518–2524.
- (57) Chae, H.; Kim, H. C.; Lee, Y. S.; Huh, S.; Kim, S. J.; et al. *Cryst. Growth Des.* **2015**, *15*, 268–277.
- (58) Kim, H. C.; Lee, Y. S.; Huh, S.; Lee, S. J.; Kim, Y. *Dalton Trans.* **2014**, *43*, 5680–5686.
- (59) Zou, C.; Zhang, Z.; Xu, X.; Gong, Q.; Li, J.; Wu, C. D. *J. Am. Chem. Soc.* **2012**, *134*, 87–90.
- (60) Alawisi, H.; Li, B.; He, Y.; Arman, H. D.; Chen, B.; et al. *Cryst. Growth Des.* **2014**, *14*, 2522–2526.